Am J Physiol Endocrinol Metab 295: E519–E530, 2008.
First published June 17, 2008; doi:10.1152/ajpendo.90436.2008.

Fetal growth restriction triggered by polycyclic aromatic hydrocarbons is associated with altered placental vasculature and *AhR*-dependent changes in cell death

Jacqui Detmar,[1,2] Monique Y. Rennie,[4,6] Kathie J. Whiteley,[1] Dawei Qu,[1] Yoshinari Taniuchi,[1] Xueyuan Shang,[1] Robert F. Casper,[1,2,5] S. Lee Adamson,[1,3,4,5] John G. Sled,[4,6] and Andrea Jurisicova[1,3,5]

[1]*Samuel Lunenfeld Research Institute, Mount Sinai Hospital, Toronto;* [2]*Institute of Medical Studies,* [3]*Department of Physiology,* [4]*Department of Medical Biophysics, and* [5]*Department of Obstetrics and Gynecology, University of Toronto, Toronto; and* [6]*Mouse Imaging Centre, Hospital for Sick Children, Toronto, Ontario, Canada*

Submitted 12 May 2008; accepted in final form 13 June 2008

Detmar J, Rennie MY, Whiteley KJ, Qu D, Taniuchi Y, Shang X, Casper RF, Adamson SL, Sled JG, Jurisicova A. Fetal growth restriction triggered by polycyclic aromatic hydrocarbons is associated with altered placental vasculature and *AhR*-dependent changes in cell death. *Am J Physiol Endocrinol Metab* 295: E519–E530, 2008. First published June 17, 2008; doi:10.1152/ajpendo.90436.2008.—Maternal cigarette smoking is considered an important risk factor associated with fetal intrauterine growth restriction (IUGR). Polycyclic aromatic hydrocarbons (PAHs) are well-known constituents of cigarette smoke, and the effects of acute exposure to these chemicals at different gestational stages have been well established in a variety of laboratory animals. In addition, many PAHs are known ligands of the aryl hydrocarbon receptor (AhR), a cellular xenobiotic sensor responsible for activating the metabolic machinery. In this study, we have applied a chronic, low-dose regimen of PAH exposure to C57Bl/6 female mice before conception. This treatment caused IUGR in *day 15.5* post coitum (d15.5) fetuses and yielded abnormalities in the placental vasculature, resulting in significantly reduced arterial surface area and volume of the fetal arterial vasculature of the placenta. However, examination of the small vasculature within the placental labyrinth of PAH-exposed dams revealed extensive branching and enlargement of these vessels, indicating a possible compensatory mechanism. These alterations in vascularization were accompanied by reduced placental cell death rates, increased expression levels of antiapoptotic Xiap, and decreased expression of proapoptotic Bax, cleaved poly(ADP-ribose) polymerase-1, and active caspase-3. *AhR*-deficient fetuses were rescued from PAH-induced growth restriction and exhibited no changes in the labyrinthine cell death rate. The results of this investigation suggest that chronic exposure to PAHs is a contributing factor to the development of IUGR in human smokers and that the AhR pathway is involved.

intrauterine growth restriction; aryl hydrocarbon receptor; murine placental vasculature

CIGARETTE SMOKING DURING PREGNANCY has serious consequences to maternal, embryonic, fetal, and neonatal health, having been associated with increased risks of spontaneous abortion, placental abruption, placenta previa, ectopic pregnancy, and premature delivery (for reviews, see Refs. 20, 43, 72). Gestational exposure to tobacco products is causally associated with intrauterine growth restriction (IUGR) and is considered the mediating factor in smoking-related neonatal mortality (4). Although the direct cellular targets of cigarette smoke causing the IUGR phenotype are unknown, maternal smoking has been reported to influence the placental architecture, affecting both the vascular and trophoblast compartments. Histomorphometric studies of placentas from smoking mothers have revealed alterations in maternal intervillous spaces (17) and fetal capillary volume (16, 17, 52) and surface area (52). Functionally, these changes appear to alter blood flow in both the uterine and umbilical placental circulations, based on Doppler studies (2, 50). Within the trophoblast compartment, maternal exposure to cigarette smoke has been associated with reduced syncytiotrophoblast apoptosis (56) and trophoblast hyperplasia (67, 81).

There are more than 4,000 chemical components found in cigarettes; however, the main toxicants are a group of carcinogens known as polycyclic aromatic hydrocarbons (PAHs) (45). Included in this group are benzo[*a*]pyrene (BaP) and 7,12-dimethylbenz[*a*]anthracene (DMBA), which are known carcinogens and whose toxic effects include the formation of DNA and protein adducts, in addition to triggering the expression of xenobiotic-metabolizing enzymes through binding to the aryl hydrocarbon receptor (AhR). Although PAHs are known environmental pollutants generated by fossil fuel combustion, car exhaust, and forest fires (38), the major source of human exposure is through the use of tobacco products (9). PAHs exert their toxic effects on a variety of organs, including those of the reproductive system (for review, see Ref. 61). Furthermore, PAHs have been shown to cross the placenta (8, 14) and form hemoglobin adducts in both maternal and fetal sera (73), in addition to forming DNA adducts in both human (37) and murine (55) trophoblast cells.

The AhR is a basic helix-loop-helix transcription factor, acting as a xenobiotic sensor for a number of different hydrocarbons, including PAHs (for review, see Refs. 18, 25). Ligands, such as BaP and DMBA, diffuse across the cell membrane and bind to AhR, causing a transformational shift and exposing a nuclear localization sequence. This allows the receptor-ligand complex to translocate into the nucleus, where it binds the AhR nuclear translocator (ARNT). The AhR-ARNT complex binds AhR/dioxin/xenobiotic response elements (AREs/DREs/XREs), activating the transcription of cellular detoxification machinery. *AhR*-deficient mice are resistant to BaP-induced carcinogenicity (71) and dioxin toxicity (15, 33) and exhibit cardiac hypertrophy, reduced fecundity, and

Address for reprint requests and other correspondence: A. Jurisicova, Samuel Lunenfeld Research Institute, Mount Sinai Hospital, 600 Univ. Ave., Toronto, ON, Canada M5G 1X5 (e-mail: jurisicova@mshri.on.ca).

The costs of publication of this article were defrayed in part by the payment of page charges. The article must therefore be hereby marked "*advertisement*" in accordance with 18 U.S.C. Section 1734 solely to indicate this fact.

postnatal growth retardation independent of exogenous ligand (70, 78). AhR expression has been previously demonstrated in the mouse uterus and fetal endothelium of the mouse placenta (51).

A number of murine studies have explored the consequences of acute dioxin or PAH exposure during gestation (41, 49, 83). In addition, laboratory studies have revealed that rats exposed to side-stream smoke during pregnancy yielded pups with significant decreases in weight (53, 63); however, there is little information regarding the effect of maternal exposure to PAHs before pregnancy. Because these chemicals have been shown to accumulate in the adipose and mammary tissue (63, 64), the slow release of unaltered PAHs into the maternal blood can still present a toxicological threat to the growing fetus. Although some studies have reported a significant association between prepregnancy exposure to tobacco products and fertility (57, 59), the impact of such exposure on fetal weight is unclear. In nonstratified data sets, the association between prepregnancy maternal smoke exposure and fetal weight is statistically insignificant (23, 31, 32); however, several groups commented on the potential for association if larger data sets were available (23) and if the data were stratified with respect to urinary cotinine (32). Thus an investigation into the potential consequences of prepregnancy exposure to PAHs on fetal weight in a more controlled setting is warranted.

We previously reported a murine model (27) designed to mimic the phenomenon observed in human populations, where women will cease smoking upon attempting, or acquiring knowledge of, conception, typically due to fetal health concerns (21, 34). In this study, we sought to investigate whether PAH exposure before pregnancy could induce placental changes, thus contributing to IUGR. In addition, we wanted to determine whether AhR was involved in this growth restriction. We presently report that chronic exposure to PAHs before gestation results in compromised maternal and fetal placental vascularization and altered labyrinthine architecture in C57Bl/6 mice, leading to IUGR. We further show that this PAH-induced IUGR is inhibited by *AhR* deficiency.

MATERIALS AND METHODS

In vivo BaP and DMBA treatment. C57Bl/6 (National Cancer Institute, Frederick, MD) and AhR heterozygous (C57Bl/6-*AhR*^{tm1Bra}) virgin female mice were randomly separated into PAH- or vehicle-treated groups and group-housed in separate cages. Animals were maintained in a controlled room with a 12:12-h light-dark cycle and allowed ad libitum access to rodent chow and water. Subcutaneous injections of vehicle (corn oil) or PAHs were administered over a 9-wk period as previously described (27). The final, cumulative dose for PAH-treated mice was 12 mg/kg; vehicle-treated animals were given proportional injections of corn oil.

Mating and tissue collection. Four days after the last injection, female mice were mated with the appropriate male stud (i.e., C57Bl/6 or AhR heterozygous). Gestational age was determined based on the presence of a vaginal plug, with the morning of detection designated as *day 0.5*. Plugged females were removed from the males and group-housed in separate cages. Only females that plugged within 4 wk after the last injection were used in this study. To evaluate late-gestational effects of PAH exposure (pups are born *day 19.0*), pregnant dams were euthanized by cervical dislocation at *day 15.5* and the number of conceptuses and resorptions was recorded. Fetuses and placentas were removed from the uterus, and wet weights were recorded. Placentas were either fixed in 10% formalin overnight or stored at −80°C. For AhR heterozygous crosses, a piece of fetal forelimb tissue was used for PCR genotyping (66). All animal experiments were conducted in accordance with the Canadian Council of Animal Care guidelines, and protocols were approved by the Animal Care Committee of Mount Sinai Hospital.

Vascular casting and ultrasound biomicroscopy. Microcomputed tomography (micro-CT) was employed to obtain quantitative measurements of the fetoplacental vasculature, using methods previously described (65). Briefly, *day 15.5* pregnant uteri from vehicle- and PAH-exposed dams were collected into ice-cold PBS. Conceptuses were individually exposed and warmed with saline to initiate cardiac function and placental blood flow. After a glass cannula was inserted into either the umbilical vein or artery, blood was flushed from the placental circulation with warmed saline (0.9% NaCl, 2% xylocaine, and 100 IU heparin/ml). Radio-opaque silicone rubber (Microfil; Flow Technology, Carver, MA) was infused into the umbilical artery or vein until it reached the capillaries. The umbilical cord was tied off, and the casting compound was allowed to polymerize for 1 h, after which the placenta was severed from the fetus. The perfused placenta was fixed in 10% phosphate-buffered formalin and mounted in 1% agar containing 10% formalin for subsequent scanning. Three-dimensional data sets were obtained using an MS-9 micro-CT scanner (GE Medical Systems, London, ON, Canada) and analyzed using Amira software (TGS, Berlin, Germany). Images and data were obtained for both arterial ($n_{vehicle}$ = 9 placentas from 4 dams; n_{PAH} = 9 placentas from 4 dams) and venous ($n_{vehicle}$ = 8 placentas from 4 dams; n_{PAH} = 8 placentas from 4 dams) fetal vessels.

Vascular corrosion casts were used to qualitatively examine the fetal and maternal placental circulations. Vehicle- and PAH-exposed C57Bl/6 pregnant dams were euthanized by cervical dislocation at *day 15.5*, and vascular corrosion casts were made with methyl methacrylate (i.e., plastic) casting compound (Batson's no. 17; no. 07349; Polysciences, Warrington, PA) and processed for scanning electron microscopy using established methods (1). Plastic casts of the fetal ($n_{vehicle}$ = 4 placentas from 2 dams; n_{PAH} = 5 placentas from 2 dams) and maternal ($n_{vehicle}$ = 3 placentas from 2 dams; n_{PAH} = 3 placentas from 2 dams) placental circulations were viewed using a FEI XL30 (FEI Systems Canada, Toronto, ON, Canada) scanning electron microscope.

Ultrasound biomicroscopy was utilized to assess placental hemodynamics and fetal dimensions in vivo. Vehicle- and PAH-exposed dams were anesthetized with isoflurane at *day 15.5*. Fetal crown-rump length, heart rate, and blood velocity in the umbilical artery were measured noninvasively using 30-MHz ultrasonography (Vevo 770; Visualsonics, Toronto, ON, Canada). Data were obtained for 11–15 fetuses from 3 vehicle-exposed dams and 17–19 fetuses from 4 PAH-exposed dams.

Terminal deoxynucleotidyl transferase dUTP nick-end labeling. C57Bl/6, AhR wildtype (WT), and AhR knockout (KO) placentas from vehicle- or PAH-exposed dams were embedded in paraffin using routine histological techniques, and 5-μm sections were taken at the midline. Sections were deparaffinized and treated with 10 μg/ml proteinase K (no. 25530015; Invitrogen, Burlington, ON, Canada) in PBS for 13 min, followed by brief washes with MilliQ water and PBS. Endogenous peroxidase was quenched in 3% H_2O_2 in methanol, and slides were washed and incubated for 90 min at 37°C in terminal deoxynucleotidyl transferase dUTP nick-end labeling (TUNEL) mixture containing 1× One-Phor-All *PLUS* buffer, 10 μM biotin-16-dUTP (no. 1093070; Enzo Life Sciences, Farmingdale, NY), 1 μM dATP (no. R0181; Fermentas, Burlington, ON, Canada), and 20 IU of terminal deoxynucleotidyl transferase, FPLC pure enzyme (no. 27-0730-01; GE Healthcare, Baie d'Urfe, QC, Canada). Streptavidin-horseradish peroxidase reagent (no. PK-4000; Vector Laboratories, Burlingame, CA) was used for detection of incorporated nucleotides, and the color reaction was developed using 3,3′diaminobenzidine (DAB) substrate (no. D5905; Sigma). Sections were counterstained with methyl green, dehydrated, and mounted. Histomorphometric analyses were done on each placental section using a Zeiss 9901

microscope, a Retiga 1300 camera, and BioQuant software. Placental layers were divided into labyrinthine, junctional zone (area between the labyrinth and giant cell layers), and maternal compartment layers (area between the giant cell layer and the myometrium); measurements also included the yolk sac and allantoic mesenchyme (YSAM) of the chorionic plate. Tissue areas were determined at ×25, ×100, or ×500 magnification, and TUNEL-positive cells were counted at ×500 magnification, with each section scanned in its entirety. Focal regions of cell death in the maternal compartment were defined as a group of 10 or more TUNEL-positive cells. These regions were quantified as the percent area of TUNEL positivity over the total area of tissue in the maternal compartment. Photomicrographs were taken using a Leitz DMRXE microscope, a Sony DXC-970MD camera, and Northern Eclipse software.

Histological staining. Sections were deparaffinized in xylene and rehydrated to water. To distinguish cytotrophoblast cells lining the maternal blood spaces, rehydrated sections were briefly equilibriated with alkaline phosphatase (AP) buffer (100 mM Tris, 100 mM NaCl, and 5 mM $CaCl_2$, pH 8.5) and then held in AP substrate solution (nitro blue tetrazolium + 5-bromo-4-chloro-3-indolyl phosphate in AP buffer; no. S3771; Promega, Madison, WI) for 25 min at 37°C in a humidified chamber. Slides were washed briefly with water, stained with nuclear fast red, and counterstained with 1% tartrazine yellow. To visualize collagen deposition, rehydrated sections were postfixed in Zenker's fixative for 1 h and processed for Masson's trichrome stain using routine histological methods.

Immunohistochemistry and lectin histochemistry. Sections were deparaffinized in xylene, rehydrated, and underwent microwave antigen retrieval in 10 mM citrate buffer, pH 6.0. Sections were allowed to cool down to room temperature, washed, and then blocked with 10% horse serum plus 10% BSA in PBS with 0.1% Tween 20 (PBST). Anti-AhR antibody (1:500; no. SA-210; Biomol, Plymouth Meeting, PA) was diluted 1:500 in 5% horse serum plus 5% BSA in PBS. Slides were then held at 4°C overnight and washed in PBS, followed by a 2-h incubation at room temperature with biotinylated anti-rabbit antibody (1:200 dilution in 5% horse serum + 5% BSA) from a VectaStain ABC kit (no. PK-4001, Vector Laboratories). The ABC solution was prepared according to the manufacturer's instructions, and detection using DAB substrate was done as described above, followed by counterstaining with hematoxylin. Cells were considered positive for AhR expression if they stained positive in AhR WT placentas and were negative in placentas from *AhR*-deficient littermates. Determination of cell type (i.e., trophoblast vs. endothelial) was based on location of the cell within the tissue and cellular/nuclear morphology.

Lectin histochemical methods were similar to those described for immunohistochemistry, except antigen retrieval was omitted and secondary antibody was not needed. Instead, sections were blocked and subsequently probed with 50 μg/ml biotinylated *Bandeiraea simplicifolia* (BS-I; no. L3759; Sigma) for 1 h at room temperature, followed by peroxidase quenching using 1% H_2O_2 in PBS. Detection of reaction using the ABC complex and DAB substrate was done as described above. Images of sections after immunohistochemistry and lectin histochemistry were taken using the same instrumentation as that described for TUNEL photomicrography.

Caspase-3 enzyme assay. Enzymatic activity of caspase-3 in murine placental tissues was assessed using the Caspase-3 Cellular Activity Assay Kit PLUS (no. AK-004; Biomol, Plymouth Meeting, PA). Briefly, *day 15.5* placentas (1 placenta from each of $n = 4$ dams) were dissected into maternal enriched (i.e., mainly decidua) and fetal enriched (i.e., mainly trophoblast giant cells, spongiotrophoblast, and labyrinth) fractions. These were then weighed and homogenized in cell lysis buffer. Protein concentration was determined using the Bradford assay (no. 500-0006EDU; Bio-Rad, Mississauga, ON, Canada). Thereafter, the assay was performed according to the manufacturer's protocol using the colorimetric pNA substrate provided. Absorbance readings were obtained using a μQuant microtiter plate reader (Molecular Devices, Sunnyvale, CA), with readings taken every 10 min for a total of 120 min. Calculation of enzymatic activity was done using the slope of the linear portion of the time course.

Western blotting. To assess protein expression in control or treated *day 15.5* C57Bl/6 placentas, one placenta from each of five dams was placed in PBS containing a Complete protease inhibitor tablet (no. 1836170; Roche, Laval, QC, Canada), weighed, and placed on ice. Individual AhR WT and KO placentas (vehicle and PAH exposed) were similarly treated after removal of maternal decidua. The tissue was homogenized in 1× SDS sample buffer, and DNA was sheared by passing the sample several times through a 23.5-gauge needle. Samples were then held at 100°C for 3 min, allowed to cool, and centrifuged briefly. Standard denaturing acrylamide gels of varying concentrations were prepared according to the manufacturer's instructions (Novex). Proteins were transferred to 0.2-μm BioTrace nitrocellulose (no. 66485; Pall, Mississauga, ON, Canada). Blots were blocked for 1 h with 5% skim milk in Tris-buffered saline (TBS) with 0.1% Tween 20 (TBST) for 1 h. The following primary antibodies were used: anti-caspase-3 (1:500; no. 9662; Cell Signaling, Danvers, MA), anti-cleaved Parp-1 (1:500; no. 9544; Cell Signaling), anti-Bax NT (1:500; no. 06-499; Upstate, Lake Placid, NY), anti-Xiap (1:500; no. 610762; BD Biosciences, Mississauga, ON, Canada), anti-CYP1A1 (1:400; no. A3001; Xenotech, Lenexa, KS), anti-CYP1B1 (1:400; no. 458511; Gentest, Woburn, MA), anti-FasL (1:200; no. PC78; Calbiochem, Mississauga, ON, Canada), anti-PTEN (1:500; no. 9559; Cell Signaling), anti-p21 (1:100; no. 554085; BD Biosciences), and anti-FAK (1:100; no. sc-558; Santa Cruz Biotechnology, Santa Cruz, CA). Blots were stripped and reprobed with anti-β-actin antibody (1:400; no. sc-1616, Santa Cruz Biotechnology) to correct for protein loading. Membranes were incubated with ECF substrate (enhanced chemifluorescence, no. RPN5785; GE Healthcare) and scanned on a STORM imager (Molecular Devices). Densitometric analyses were done using ImageQuant software.

Statistical analysis. Statistical analysis of AhR data was done using two-way ANOVA. All other statistical tests were done using Student's *t*-test. Statistical software used was SPSS (version 13), and changes were considered statistically significant if $P \leq 0.05$.

RESULTS

Maternal exposure to PAHs before conception leads to IUGR and altered labyrinthine vasculature in C57Bl/6 mice. Previously, we reported that PAH-exposed dams on an outbred, ICR genetic background exhibited high rates of embryonic resorption early in gestation (27). However, when the same dosing regimen was applied to an inbred, C57Bl/6 genetic background, dams yielded fetuses with a 14% reduction in weight compared with fetuses from dams exposed to vehicle (Fig. 1*A*). These data were supported by crown-rump length measurements by ultrasound biomicroscopy, which were significantly reduced in fetuses from PAH-exposed dams (Fig. 1*B*); however, fetal abdominal cross-sectional area was unaltered with PAH exposure. C57Bl/6 females exposed to PAHs exhibited no difference in the number of fetuses per litter compared with dams exposed to vehicle (7.8 ± 0.3 pups per litter, $n_{vehicle} = 11$ dams; 7.2 ± 0.52 pups per litter, $n_{PAH} = 11$ dams; $P = 0.30$).

Evaluation of *day 15.5* placental sections using various histological techniques revealed aberrations in the labyrinthine region, particularly in the vasculature. After placental sections from PAH-exposed dams were stained with Masson's trichrome, it was apparent that collagen deposition along the chorionic plate and into the large allantoic vessels was thinner than in vehicle-treated controls (Fig. 1*C*). In addition, AP and lectin histochemistry (markers of maternal and fetal blood spaces, respectively) revealed alterations in the labyrinthine architecture

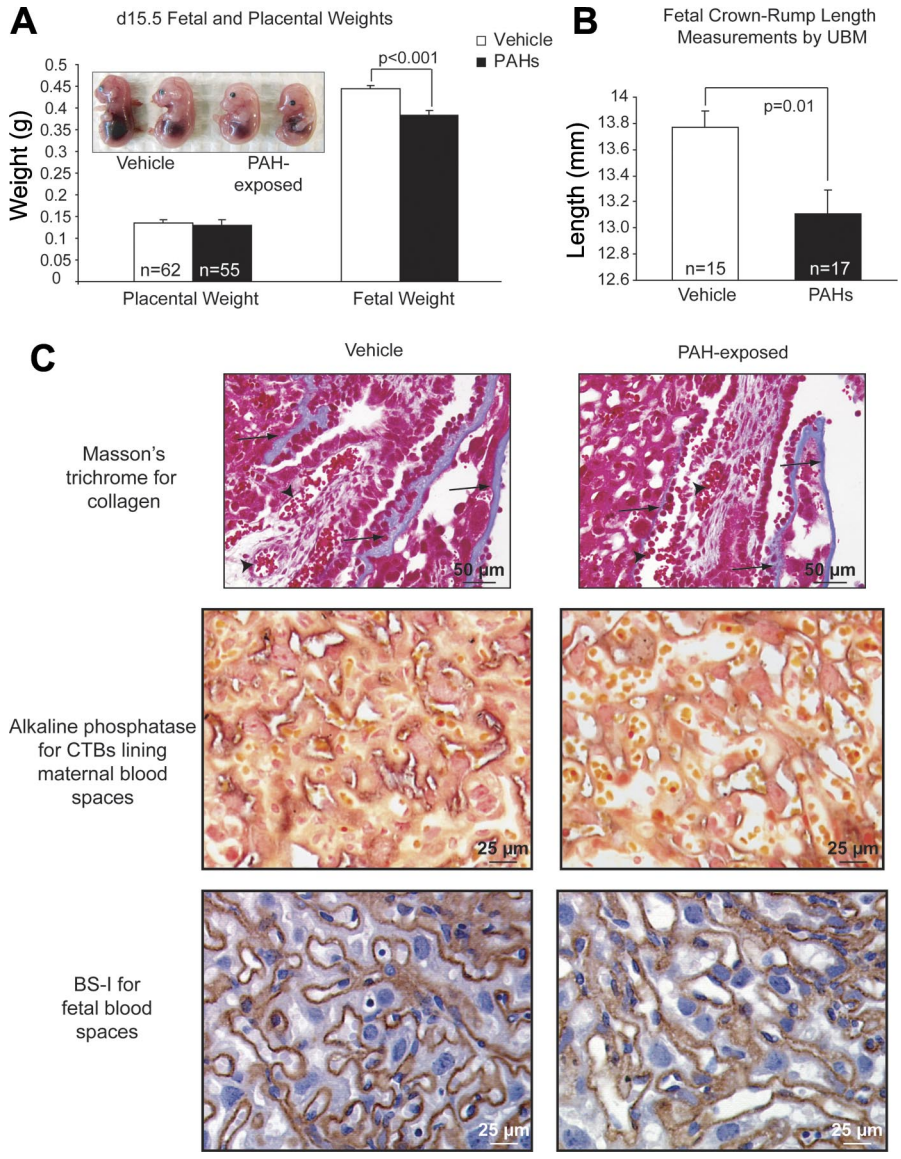

Fig. 1. Maternal exposure to PAHs prior to conception leads to IUGR and altered labyrinthine architecture in d15.5, C57Bl/6 placentae. Bar graph depicts placental and fetal weight of d15.5 conceptuses from C57Bl/6 dams exposed to vehicle (n = 62 conceptuses from 8 dams) or PAHs (n = 55 conceptuses from 8 dams) prior to pregnancy. Inset photograph depicts representative fetuses from a vehicle-exposed (two fetuses at left) and PAH-exposed dam (two fetuses at right). (*B*) Graph demonstrates fetal crown-rump length measurements of d15.5 fetuses from vehicle-exposed (n = 15 fetuses from 3 dams) and PAH-exposed (n = 17 fetuses from 4 dams) dams. (*C*) Photomicrographs in upper panel represent the lateral edge of d15.5 placentae, exposed to vehicle or PAHs and stained with Masson's trichrome (nuclei are dark red-blue, cytoplasm is red, collagen is bright blue). Decreased collagen deposition at chorionic plate was observed in 8/10 placental sections from n = 5 PAH-exposed dams. Photomicrographs in middle panel are of d15.5 placental labyrinth obtained from vehicle- or PAH-exposed dams, after histochemical staining with alkaline phosphatase (AP) and counterstaining with nuclear fast red and tartrazine yellow. Purple-staining outlines the maternal blood spaces due to fetal cytotrophoblast reaction with AP substrate, cytoplasm is yellow or yellow-orange and nuclei are red. Diminished alkaline phosphatase staining was observed in 8/10 placental sections from n = 5 PAH-exposed dams. Lower panel contains photomicrographs of d15.5 C57Bl/6 labyrinth exposed to vehicle or PAHs and labeled with BS-I lectin (a marker of endothelial cells), outlining the fetal blood spaces; nuclei are counterstained with hematoxylin. Enlargement and disorganization of labyrinthine vessels was observed in 10/10 placental sections from n = 5 PAH-exposed dams. Bars represent mean values ± standard error (SE) and values of significant statistical difference are shown with the corresponding p value. Arrows indicate the line of collagen deposition at the chorionic plate, arrowheads indicate fetal vessels and asterisks indicate maternal blood spaces.

characterized by enlargement of both the maternally perfused sinusoids and the fetal capillaries (Fig. 1*C*). The other placental regions were also examined but did not exhibit any obvious defect.

To evaluate more global changes in the maternal and fetal vasculatures, we examined placental vascular corrosion casts by scanning electron microscopy. Consistent with the alterations observed in histological sections, placental vascular casts revealed that the fetal labyrinthine capillaries in mothers treated with PAHs consistently appeared enlarged relative to those in dams exposed to vehicle (Fig. 2*A*). In addition, PAH-exposed fetal capillaries exhibited a greater number of intricate anastomses and a greater degree of tortuosity compared with the more linear structures observed in the fetal casts exposed to vehicle (Fig. 2*A*). These alterations in the tortuosity of the capillary network in PAH-exposed placentae were especially striking in those vessels running along the approximate midline of the villous tree. With respect to the maternal contribution of placental blood, the labyrinthine sinusoids of PAH-exposed placentas also appeared enlarged in a manner similar to that seen in the fetal-side casts (Fig. 2*B*). Finally, large, maternal arterial canals were consistently (3/3 placentas examined) observed close to the chorionic surface of placentas obtained from dams treated with PAHs (Fig. 2*B*).

Reduced umbilical vessel diameter and total fetoplacental vascular surface area and volume in day 15.5 placentas from PAH-exposed dams. Microcomputed tomography was employed to examine fetoplacental vessels >0.03 mm (i.e., excludes capillaries). The acquired surfaces (see Fig. 3, *A* and *C*) allowed three-dimensional visualization of the fetoplacental vasculature as well as calculation of vessel diameters, surface area, and overall lumen volume. Although no overt changes in the large vessels (i.e., >30 μm) of the venous vasculature were observed between vehicle- and PAH-exposed placentae, the arterial surface renderings of PAH-exposed placentas displayed a greater degree of tortuosity in some large vessels of the trees (Fig. 3*B*). In addition, PAH-exposed placentas exhibited significantly reduced arterial surface area and volume compared with placentas from vehicle-exposed dams (Fig. 3, *D* and *E*). No change in venous surface area or volume was

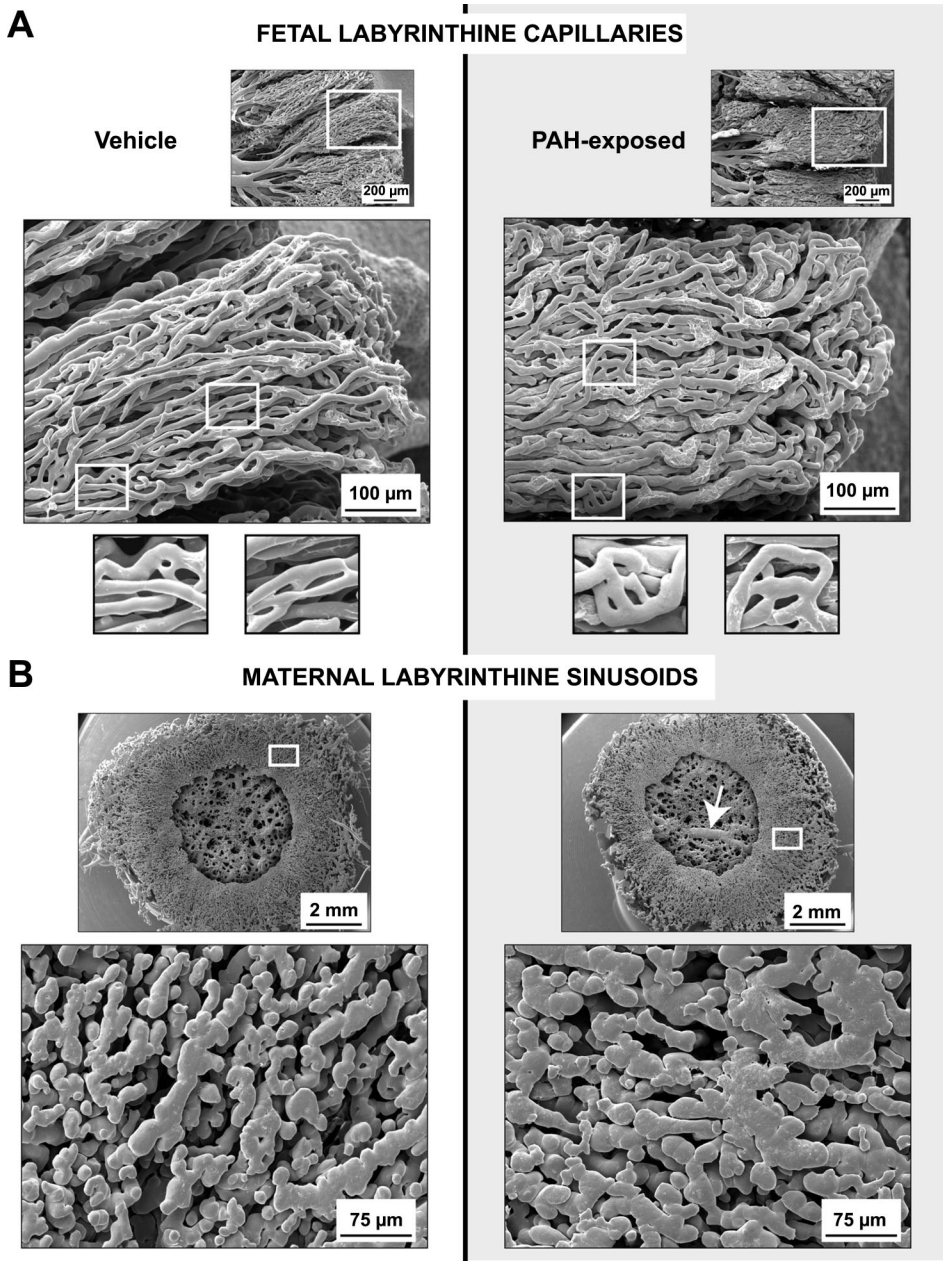

Fig. 2. Maternal exposure to PAHs prior to conception in C57Bl/6 mice results in aberrant placental microvasculature in both the fetal and maternal compartments. (*A*) Scanning electron photomicrographs of corrosion casts of fetal labyrinthine capillaries from vehicle and PAH-exposed d15.5 C57Bl/6 placentae. Boxed region in the upper panel is magnified in the middle panel. Boxed regions in the middle panel are magnified in the lower panel (scale bar = 10 μm). These regions depict representative examples of the higher degree of branching, anastomosing and tortuosity observed in the fetal labyrinthine vessels of PAH-exposed placentae. (*B*) Corrosion casts of maternal labyrinthine sinusoids from vehicle and PAH-exposed d15.5 placentae. Boxed region in upper panel is magnified in lower panel. Arrow indicates large, exposed maternal arterial canal that were consistently observed (in 3/3 placentae examined from $n = 2$ PAH-exposed dams) in maternal vasculature casts obtained from PAH-exposed dams.

observed between the two groups; however, both the umbilical artery and vein demonstrated significant decreases in diameter in placentas from dams treated with PAHs compared with dams treated only with vehicle (Fig. 3*F*). However, PAH exposure did not effect changes in fetal heart rate and umbilical artery peak velocity, as determined by Doppler studies (data not shown).

Both fetal and maternal compartments of day 15.5 PAH-exposed placentas exhibit altered cell death rates and changes in cell death markers. PAHs have been implicated in altering the balance of cell survival and death in a number of different cell types (11, 12, 28). Because precisely regulated cell death is essential for trophoblast turnover, analyses of cell death were implemented. Morphometric analyses of *day 15.5* placental sections after TUNEL revealed significant decreases in the number of labeled cells in the labyrinth and junctional zone of placentas from PAH-exposed dams (Fig. 4*B*). Based on the location and the presence of fetal red blood cells, the dead/dying cells appear to be a combination of fetal endothelium and syncytiotrophoblast cells. In addition, the incidence of sporadic decidual cell death and the percent area of TUNEL-positive tissue in the maternal compartment also significantly decreased compared with placentas exposed to vehicle only (Fig. 4*C*). Conversely, PAH treatment caused a significant increase in the number of TUNEL-positive cells in the YSAM (Fig. 4*D*), whereas trophoblast giant cell death appeared unaffected.

Assessment of cell death markers revealed altered expression and activity in several key proteins. Decreased rates of placental cell death in dams exposed to PAHs were accompanied by diminished caspase-3 enzyme activity (Fig. 5*A*). These data were supported by immunoblotting, since levels of cleaved caspase-3 also declined significantly, whereas total

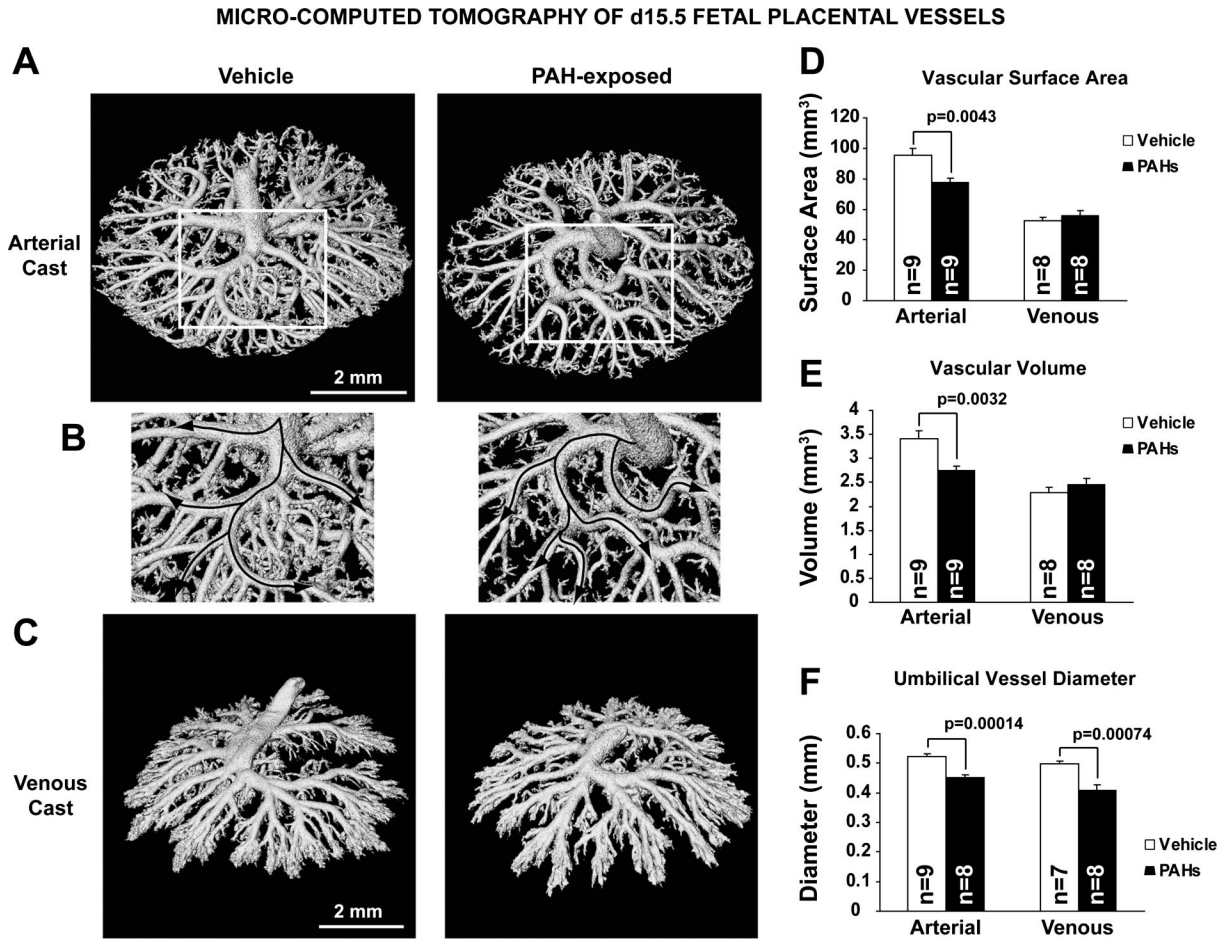

Fig. 3. Microcomputed tomography of fetal placental casts reveals decreased arterial surface area and umbilical vessel diameter in placenta from PAH-exposed C57Bl/6 dams. (*A*) Two-dimensional rendering of fetal arterial cast obtained from d15.5 placentae of vehicle and PAH-exposed dams. (*B*) Higher magnification of boxed region in (*A*) demonstrating the altered curvature of the larger fetal vessels. Arrows indicate the direction of blood flow. (*C*) Two-dimensional rendering of fetal venous cast obtained from d15.5 placentae of vehicle and PAH-exposed dams. (*D*) Graph depicting the average surface area of the fetal, arterial or venous vasculature in vehicle and PAH-exposed placentae. (*E*) Graph depicting the average fetal, arterial or venous volume in vehicle and PAH-exposed placentae. (*F*) Graph depicting the average fetal arterial or venous umbilical vessel diameter in vehicle or PAH-exposed placentae. Bars represent average values ± SE and values of significant statistical difference are shown with the corresponding p value. Note that n values reflect the number of placentae from $n_{vehicle} = 4$ or $n_{PAH} = 4$ dams.

caspase-3 levels appeared unchanged (Fig. 5*B*). Moreover, examination of the cleavage profiles of known, intracellular caspase-3 substrates (36, 79, 85) revealed significantly reduced levels of the cleaved forms of Parp-1 (Fig. 5*C*), p21, PTEN, and focal adhesion kinase (FAK) (data not shown). In addition, Bax, a proapoptotic protein known to be upregulated by AhR after PAH exposure in the ovary (58), exhibited significantly decreased levels of expression in placentas from PAH-exposed compared with vehicle-exposed dams (Fig. 5*D*). Moreover, significantly higher expression levels of Xiap, an antiapoptotic protein, were observed in placentas from PAH-treated dams (Fig. 5*E*). Finally, expression levels of FasL, previously shown to be regulated by AhR (74) and to be cytoprotective in endothelial cells (77, 87), were increased in response to PAH exposure in *day 15.5* placental lysates (Fig. 5*F*).

AhR-deficient fetuses exhibit no further growth restriction due to chronic maternal exposure to PAHs. The aryl hydrocarbon receptor acts as an intracellular sensor, triggering the transcription of cellular machinery and initiating the appropriate response against potentially harmful xenobiotics. Levels of AhR expression as determined by immunoblotting exhibited an 81% increase (see Fig. 6*A*) in WT placentas from PAH-exposed dams compared with WT placentas from dams exposed to vehicle. Furthermore, immunoblotting and densitometric analyses of PAH-exposed placental lysates exhibited significantly increased levels of the AhR-regulated proteins CYP1A1 and CYP1B1 (Fig. 6*A*). To ascertain which placental cell types express AhR, we performed immunohistochemistry on *day 15.5* placental sections. This technique revealed that AhR localized to the fetal endothelium of the labyrinthine, allantoic, and vitelline vessels. This staining pattern was specific, since it was not evident in the placentas of *AhR*-deficient littermates (Fig. 6*B*). Since AhR shares a binding partner (ARNT) with hypoxia-inducible factor (HIF)-1α, we performed Western blotting to assess whether dysregulated expression of this transcription factor contributed to the observed placental pathologies; however, no changes in HIF-1α levels were observed in placental lysates from PAH-exposed dams ($P = 0.27$; $n_{vehicle} = 4$ placentas from 4 dams; $n_{PAH} = 5$ placentas from 5 dams).

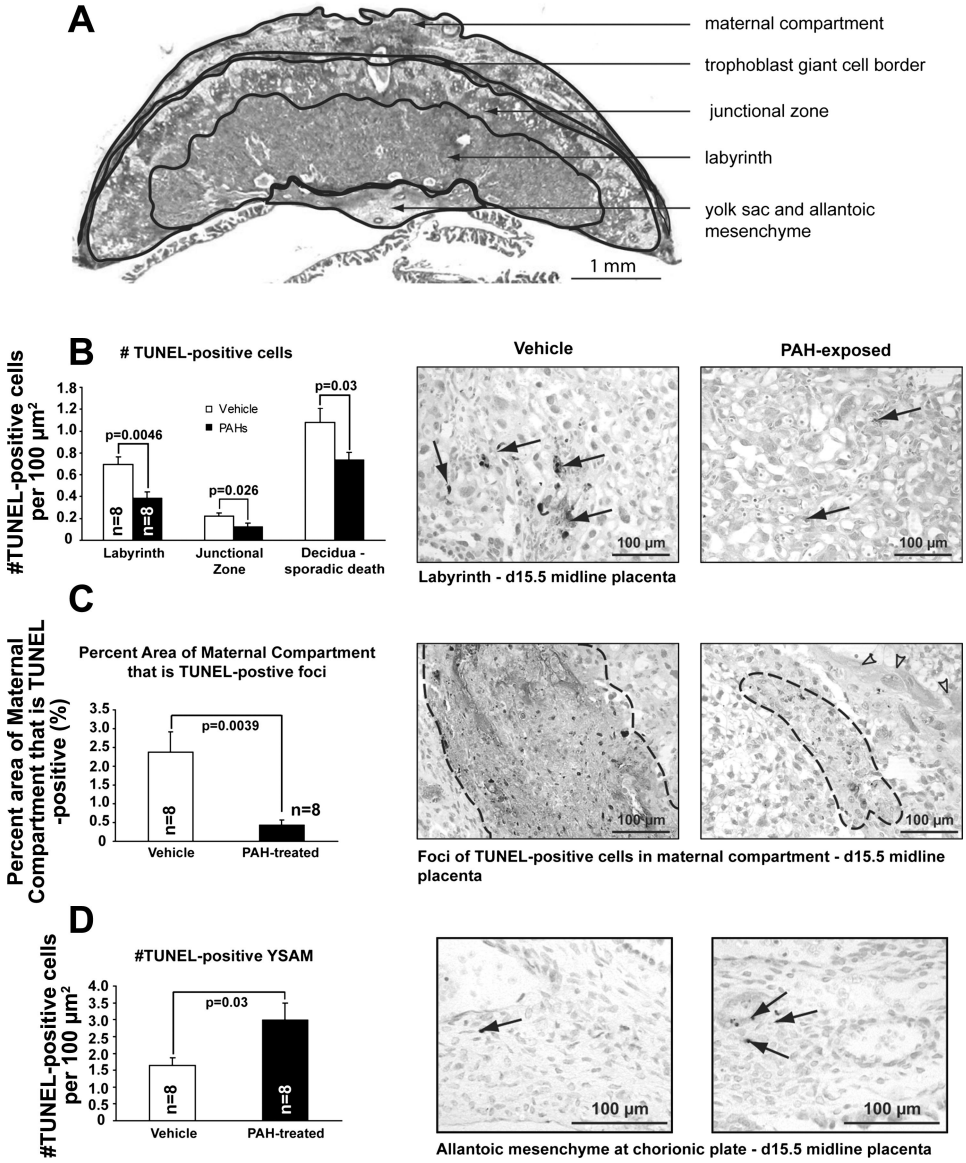

Fig. 4. Chronic exposure to PAHs prior to pregnancy leads to altered cell death patterns in d15.5 placentae of C57Bl/6 dams. (*A*) Mid-line section of d15.5 C57Bl/6 placentae stained with Masson's trichrome, indicating the regions of measurement for histomorphometric analyses. (*B*) Graph depicts the number of TUNEL-positive nuclei per 100 μm^2 of labyrinthine, junctional zone or decidual tissue in d15.5 vehicle or PAH-exposed placentae. Data for decidual cells reflect positive cells sporadically placed within the maternal compartment. Accompanying photomicrographs in right panel represents TUNEL patterns observed in vehicle or PAH-exposed placental labyrinth. (*C*) Graph depicts the percent area of tissue in the maternal compartment that was regions of clustered TUNEL-positive cells. Accompanying photomicrographs in right panel demonstrates foci - demarcated with dashed line - of TUNEL-positive cells in the maternal compartment. (*D*) Graph depicts the number of TUNEL-positive nuclei per 100 μm^2 of the YSAM in d15.5 vehicle or PAH-exposed placentae. Accompanying photomicrographs in right panel demonstrate TUNEL staining observed in vehicle or PAH-exposed YSAM. Arrows indicate TUNEL-positive nuclei and empty arrowheads specify trophoblast giant cells in the fetal compartment. Bars represent average values ± SE and values of significant statistical difference are shown with the corresponding p value. Note that n values reflect the total number of placentae evaluated (i.e., 2 placentae from each of $n_{vehicle}$ = 4 or n_{PAH} = 4 dams).

To determine whether AhR is involved in the IUGR phenotype triggered by PAH exposure, we compared birth weights of AhR WT and KO siblings. WT and heterozygous fetuses from PAH-exposed dams exhibited significantly decreased weight compared with vehicle-exposed fetuses; however, AhR KO littermates displayed no further restriction in growth compared with KO offspring from dams exposed to vehicle only (Fig. 6*C*). In addition, to determine the level of AhR activation, we evaluated placental lysates from WT and KO fetuses for CYP1A1 expression. Whereas PAH-exposed AhR WT placentas exhibited a 94% increase in CYP1A1 expression ($P = 0.04$, $n = 3$ placentas from 3 dams), PAH-exposed *AhR*-deficient placentas did not exhibit this same trend ($P = 0.37$, $n = 3$ placentas from 3 dams).

The aryl hydrocarbon receptor has been implicated in a number of different cellular pathways, including cell death, survival, and the cellular stress response. Morphometric analyses of TUNEL-stained placentas from AhR WT and KO littermates of dams exposed to vehicle or PAHs revealed a reduction in labyrinthine cell death rates of PAH-exposed AhR WT placentas, which was not evident in AhR KO placentas (Fig. 6*D*). In addition, both AhR WT and KO placentas from PAH-exposed females demonstrated significantly higher numbers of TUNEL-positive cells in the YSAM compared with that seen in AhR WT and KO placentas from dams treated with vehicle (Fig. 6*D*).

DISCUSSION

Cigarette smoking during pregnancy is linked with a number of detrimental outcomes and has now been established to be causally associated with IUGR (4). We recently reported the development of a new animal model of prepregnancy exposure to PAHs, which on an outbred genetic background (ICR) compromises preimplantation development, leading to embryonic resorptions (27). The mechanism by which PAHs exert this phenotype involves the induction of cell death in a Bax-dependent manner, since *Bax*-deficient embryos are protected

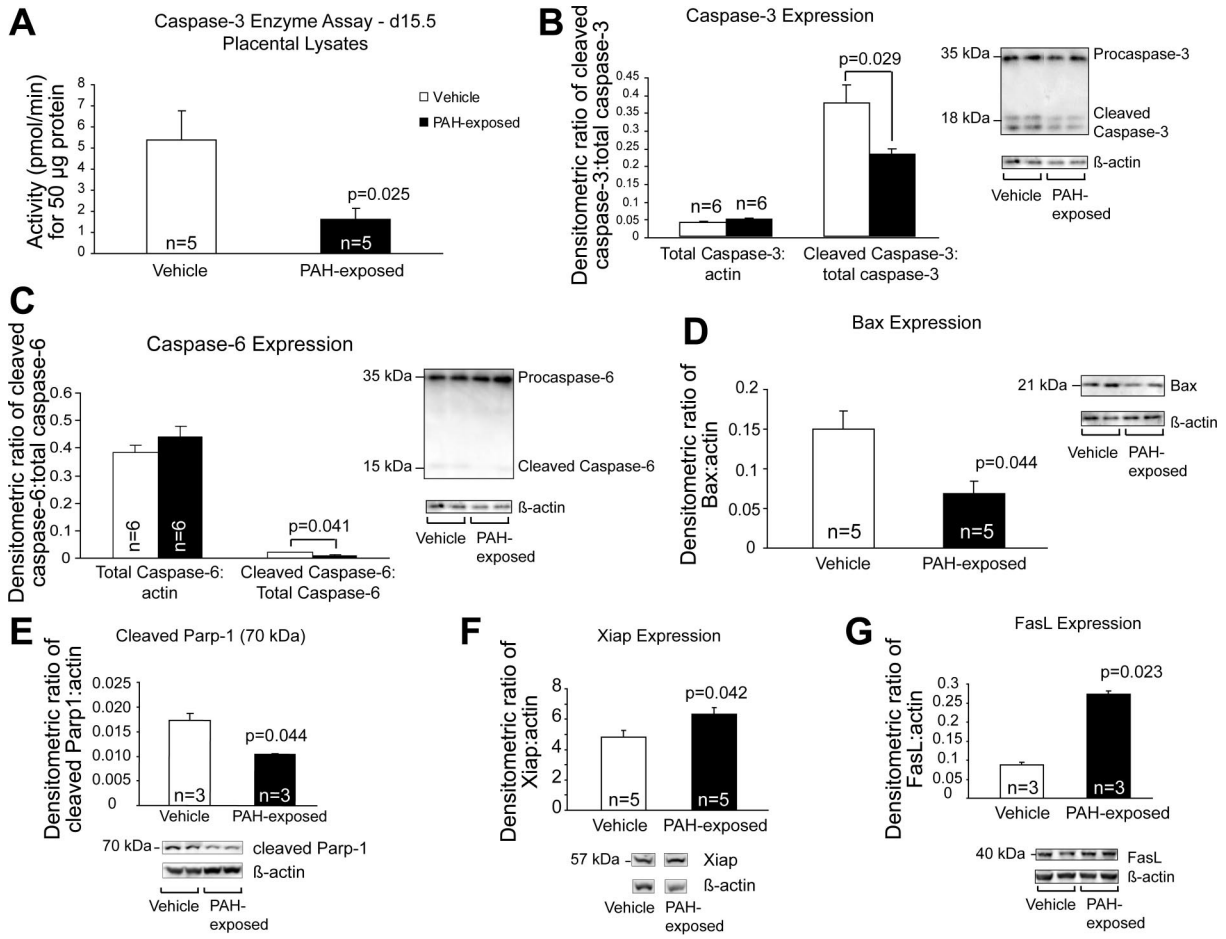

Fig. 5. Chronic exposure to PAHs prior to conception disrupts the balance of apoptotic and anti-apoptotic proteins in d15.5 C57Bl/6 placentae. (*A*) Graph demonstrates the average caspase-3 enzyme activity levels in 50 µg of placental lysate obtained from d15.5 vehicle or PAH-exposed dams. Graphs *B–E* depict levels of (*B*) total caspase-3 and cleaved caspase-3; (*C*) cleaved Parp-1; (*D*) Bax; (*E*) Xiap and, (*F*) FasL, as assessed by immunoblotting, in d15.5 placental lysates from vehicle or PAH-exposed dams. Representative immunoblots are shown to the right of each graph. Bars represent average values ± SE and values of significant statistical difference are shown with the corresponding p value. Note that n values reflect the number of placentae obtained from at least three dams.

from early postimplantation embryo loss triggered by maternal exposure to PAHs. We presently report the results of our investigations into the effects of the identical toxicant regimen on an inbred genetic background (C57Bl/6). This model closely mimics those conditions in human populations where women are exposed to chemicals from cigarette smoke over a long period of time, allowing accumulation of PAHs. Upon conception, the growing fetal and placental tissues will be exposed to both metabolized and unaltered PAHs, which have been postulated to exert a variety of effects on different cell and tissue types (reviewed in Ref. 7), including human choriocarcinoma cells (90).

In the present study, maternal exposure to PAHs before conception caused fetal growth restriction in C57Bl/6 dams, as evidenced by reduced fetal weight and length. Evaluation of two-dimensional placental sections revealed morphological changes in the labyrinth that included enlargement of the maternal and fetal vasculature and decreased amounts of collagen at the chorionic plate and along the large allantoic vessels. Alterations in the labyrinthine microvasculature were confirmed by scanning electron microscopy of fetal and maternal corrosion casts, which displayed larger, engorged vessels, irregular anastomoses, and a greater degree of vascular branching and tortuosity. It is proposed that such changes in the smaller placental vasculature (i.e., capillary level) reflect adaptive changes in response to a compromised uterine environment. Interestingly, these changes are strikingly similar to the "compact type" alterations reported in casts of fetal capillaries from term placental cotyledons of smoking mothers (60). Such alterations included capillary enlargement and increased capillary tortuosity, density, and branching suggestive of adaptive measures to increase maternal-fetal exchange (60). At the present time, it is unclear how these observed changes would alter blood flow and maternal-fetal exchange. Thus investigations into the impact of the changes in placental vascular architecture are currently underway. Finally, although we did not observe any change in placental weight associated with PAH exposure, these data correspond to those observed in the population of human smokers (44, 52, 62, 69). Thus maternal administration of PAHs in mice can recapitulate the placental vascular changes triggered by smoking in humans.

The observed changes in vascular structure may be due, in part, to the effects of PAHs on the extracellular matrix, which we have shown to be affected in the placentas from exposed dams. Previous reports have shown that cultured smooth muscle cells exposed to BaP or DMBA exhibited reduced secretion

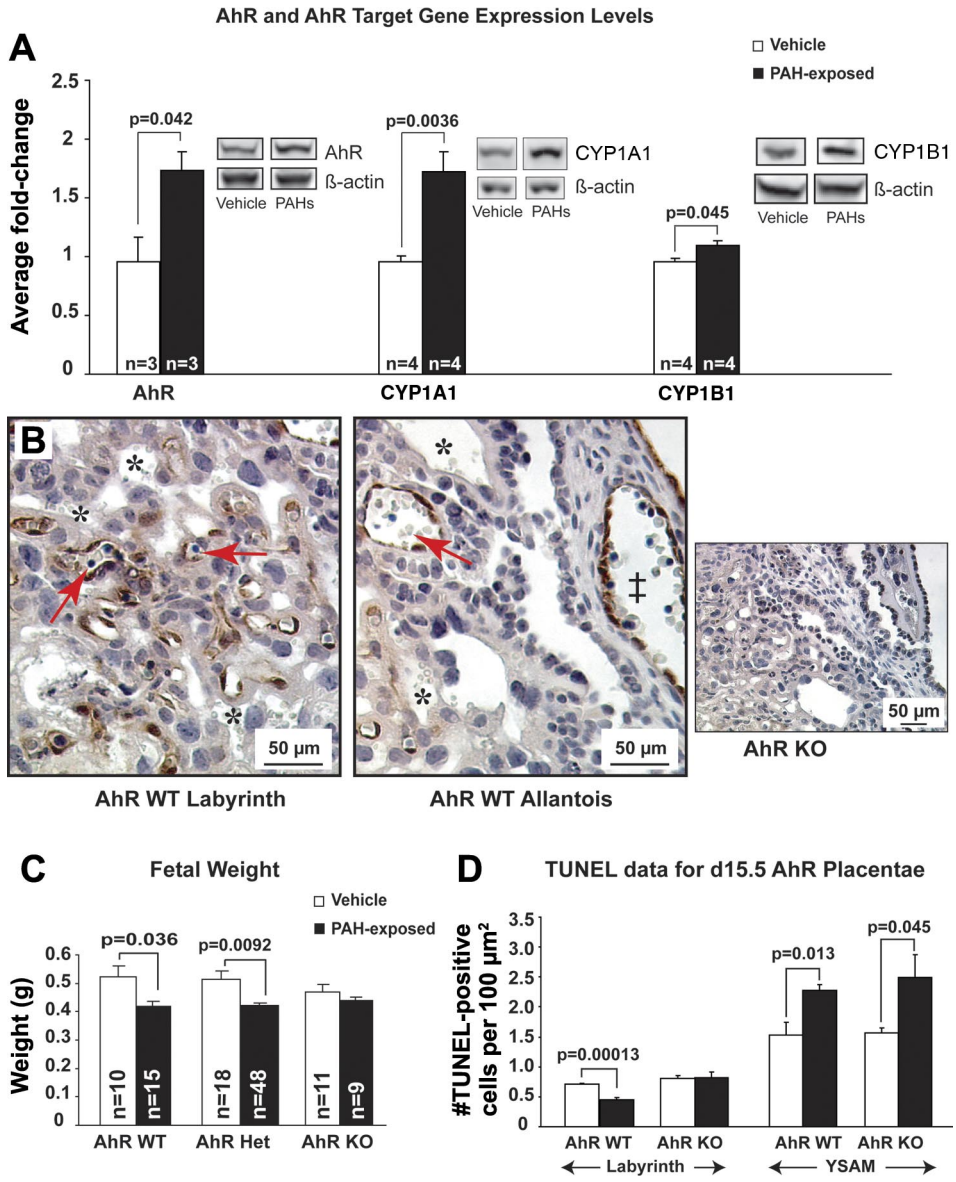

Fig. 6. Aryl hydrocarbon receptor is expressed in the fetal endothelium of the mouse placenta and *AhR* deficiency rescues the IUGR phenotype in dams chronically exposed to PAHs prior to conception. (*A*) Graph depicts the average fold-change in expression levels of AhR, CYP1A1 and CYP1B1 in d15.5 placental lysates from dams exposed to PAHs (n = 3 or 4 placentae from 3 dams) compared with placental lysates from dams exposed to vehicle (n = 3 or 4 placentae from 3 dams). (*B*) Photomicrographs of d15.5 AhR WT (left and middle panels) and AhR KO (right panel) placenta after immunohistochemical staining with anti-AhR antibody. Fetal endothelial cells in the labyrinth are indicated by arrows while those of the allantoic vasculature are indicated by a ‡. Asterisks specify maternal blood spaces. (*C*) Graph exhibits d15.5 weight in AhR WT, heterozygous and KO fetuses from heterozygous dams exposed to vehicle (n = 5 dams) or PAHs (n = 9 dams) prior to conception. (*D*) Graph depicts the average number of TUNEL-positive cells per 100 μm^2 of labyrinthine or YSAM in d15.5 AhR WT or KO placentae from dams exposed to vehicle (n_{WT} = 5; n_{KO} = 5 from 4 dams) or PAHs (n_{WT} = 5; n_{KO} = 5 from 4 dams). Bars represent average values ± SE and values of significant statistical difference are shown with the corresponding p value.

of newly synthesized collagen (75). In addition, decreased levels of type I and III procollagen, accompanied by increased matrix metalloproteinase expression, have been reported in skin fibroblasts cultured with tobacco smoke extract (88, 89). It is possible that in PAH-exposed murine placentas, expression and/or maintenance of the extracellular matrix proteins could facilitate the observed changes in vascular architecture. The significant decreases in arterial surface area and volume obtained from PAH-exposed placentas, coupled with the reduced diameters of both umbilical vessels, are predicted to negatively impact placental blood flow and/or maternal-fetal exchange. In the present study, PAH-induced changes to the large placental vessels appear profound enough to mediate IUGR, despite possible compensatory actions at the capillary level.

The importance of cell death during placental development and the consequences of disrupting this process on fetal and maternal health is highlighted by gestational diseases such as preeclampsia and IUGR (46, 76). A clear difference in cell death rates was observed in a number of PAH-exposed placental layers. Reduced levels of labyrinthine cell death were observed in our murine model, which is consistent with observations of diminished cell turnover in placentas from smoking mothers at term (39, 56). A similar reduction in trophoblast cell death was recently reported in rat placentas treated with dioxin at a late-gestational time point (47). The decline in placental cell death rates obtained in this study was supported by decreased levels of several molecular markers associated with apoptosis. In addition, PAH treatment upregulated the anti-apoptotic protein Xiap, which likely contributed to insufficient caspase-3 activity. Increased levels of Xiap were previously reported in the placentas of women smokers (39). Interestingly, although Bax levels were significantly reduced, expression of FasL was significantly higher in placentas from PAH-treated dams. Previous reports have shown that FasL is increased in endothelial cells after exposure to cigarette smoke extract (77) or ischemia-reperfusion injury (87), resulting in cytoprotection against Fas-expressing cells of the immune system. FasL is known to be regulated by AhR (74), and upregulation of this

molecule could mediate the decreased cell death rates observed in PAH-exposed placentas. Furthermore, increased expression of FasL triggered by PAH exposure may contribute to the lower incidence of preeclampsia observed in the smoking population (reviewed in Refs. 20, 29, 68), since FasL has been shown to be downregulated in this disorder (3). Finally, the significant decrease in decidual cell death may contribute to fetal growth restriction, since apoptosis facilitates maternal spiral artery remodeling (6, 40) and perturbations in this process have been associated with IUGR (reviewed in Ref. 48).

In our model of prepregnancy exposure to PAHs, placental AhR was activated, as evidenced by increased expression levels of CYP1A1 and CYP1B1, downstream targets of AhR. Labyrinthine cell death rates were not altered in PAH-exposed *AhR*-deficient fetuses, which were also rescued from the IUGR phenotype, highlighting that PAHs are responsible for this decreased apoptosis in the labyrinth, which appears to be mediated through the AhR pathway. Moreover, it appears that cell death has an important physiological function in the labyrinth, likely contributing to vascular remodeling and allowing optimal cell turnover for this metabolically active organ. On the contrary, *AhR* deficiency did not rescue the increased cell death rates observed in the YSAM, suggesting that whereas AhR mediates death in the labyrinth, another cell death pathway may be utilized in the YSAM. This curious discrepancy may reflect functional differences between the labyrinthine and YSAM endothelium, possibly through cell-to-cell signaling events. The labyrinthine endothelium is closely apposed to trophoblast-derived cells and is involved in maternal-fetal exchange. On the other hand, the endothelium of the fetal membranes and the umbilicus associates with cells originating from the allantois and lines the vessels acting as a conduit from mother to fetus. Finally, a combination of deficiencies in the extracellular matrix and increased numbers of TUNEL-positive YSAM cells after PAH exposure is predictive of a reduction in the mechanical strength of the fetal membranes. This loss of structural integrity may be responsible for the higher incidence of premature delivery and premature rupture of the membranes observed in smoking mothers (5, 84).

There is extensive phenotypic variability reported in both in vivo and in vitro studies utilizing placentae obtained from smoking mothers. The results of the present study further illustrate the necessity of considering the genetic context of observed phenotypes. Only a small proportion of women smokers exhibit IUGR, which has been associated with maternal genotype (13). We previously reported that ICR dams administered chronic doses of PAHs before conception exhibited a higher resorption rate (27)); however, placental and fetal weights did not differ between the two groups (data not shown). In the present study, we have shown that PAH-exposed C57Bl/6 dams yielded growth-restricted fetuses but no difference in resorption rate compared with dams exposed to oil. Furthermore, the majority of these mice were injected at the same time and with the same formulation, in addition to being housed in the same room, considerably reducing the number of variables between the groups. Therefore, genetic heterogeneity in human populations is likely partially responsible for the observed variability in pregnancy-related complications due to cigarette smoking. Finally, labyrinthine cell death patterns and proapoptotic Bax protein expression profiles are intriguingly different in ICR and C57Bl/6 placentas (26). This may be a contributing factor in the PAH-associated discrepancies observed in the two different strains; however, further investigation into whether AhR is directly mediating *Bax* expression after PAH exposure is required.

Another confounding issue in studying the effects of cigarette smoke in human populations is the broad variability in measuring the extent of this exposure. Self-reporting of smoking behavior in pregnant women has been shown to impart a certain degree of bias (30, 35), because some women who smoke falsely report a "nonsmoking" status (54). In addition, although testing for carbon monoxide and cotinine (a metabolite of nicotine) levels can more accurately reflect exposure to tobacco smoke, these tests have been shown to be problematic in pregnant women (42, 80) because of their higher capacity for nicotine metabolism (24). These issues underscore the need for a satisfactory animal model to elucidate the affected molecular pathways upon PAH exposure before and during gestation. Although there are differences between murine and human placentation, there are striking similarities in placental cell lineage, tissue organization, and gene expression profiles (19, 22). As such, the mouse placenta has proven to be a useful animal model in dissecting developmental pathways and directing investigators toward meaningful interpretation of human placental pathologies.

Our murine model of PAH exposure during pregnancy recapitulates a number of conditions reported in the human literature (20, 39, 43, 72). These include alterations in placental vasculature, IUGR, and altered cell death patterns observed in C57Bl/6 mice (this study) and increased rates of spontaneous abortion in ICR mice (27). Finally, this murine model of PAH exposure during pregnancy would be valuable to assess the effects of gestational exposure to environmental pollutants, many of which trigger the AhR pathway (reviewed in Ref. 61). Both epidemiological and clinical studies have reported deleterious reproductive outcomes such as low birth weight, sudden infant death syndrome, and neonatal mortality associated with exposure to environmental pollution (10, 82, 86).

GRANTS

This work was supported by research grants from the Canadian Institute of Health Research (CIHR) and the Canadian Tobacco Control Research Initiative. During these studies, J. Detmar was funded by a Doctoral Research Award from the National Sciences and Engineering Research Council, and A. Juriscova was funded by a CIHR salary award. S. L. Adamson is the Anne and Max Tanenbaum Chair in Molecular Medicine.

DISCLOSURES

S. L. Adamson previously consulted for VisualSonics.

REFERENCES

1. **Adamson SL, Lu Y, Whiteley KJ, Holmyard D, Hemberger M, Pfarrer C, Cross JC.** Interactions between trophoblast cells and the maternal and fetal circulation in the mouse placenta. *Dev Biol* 250: 358–373, 2002.
2. **Albuquerque CA, Smith KR, Johnson C, Chao R, Harding R.** Influence of maternal tobacco smoking during pregnancy on uterine, umbilical and fetal cerebral artery blood flows. *Early Hum Dev* 80: 31–42, 2004.
3. **Allaire AD, Ballenger KA, Wells SR, McMahon MJ, Lessey BA.** Placental apoptosis in preeclampsia. *Obstet Gynecol* 96: 271–276, 2000.
4. **Ananth CV, Platt RW.** Reexamining the effects of gestational age, fetal growth, and maternal smoking on neonatal mortality. *BMC Pregnancy Childbirth* 4: 22, 2004.
5. **Andres RL, Day MC.** Perinatal complications associated with maternal tobacco use. *Semin Neonatol* 5: 231–241, 2000.

6. **Ashton SV, Whitley GS, Dash PR, Wareing M, Crocker IP, Baker PN, Cartwright JE.** Uterine spiral artery remodeling involves endothelial apoptosis induced by extravillous trophoblasts through Fas/FasL interactions. *Arterioscler Thromb Vasc Biol* 25: 102–108, 2005.
7. **Baird WM, Hooven LA, Mahadevan B.** Carcinogenic polycyclic aromatic hydrocarbon-DNA adducts and mechanism of action. *Environ Mol Mutagen* 45: 106–114, 2005.
8. **Barbieri O, Ognio E, Rossi O, Astigiano S, Rossi L.** Embryotoxicity of benzo(*a*)pyrene and some of its synthetic derivatives in Swiss mice. *Cancer Res* 46: 94–98, 1986.
9. **Becher G, Bjorseth A.** Determination of exposure to polycyclic aromatic hydrocarbons by analysis of human urine. *Cancer Lett* 17: 301–311, 1983.
10. **Bobak M, Leon DA.** Air pollution and infant mortality in the Czech Republic, 1986–88. *Lancet* 340: 1010–1014, 1992.
11. **Bohnenberger S, Wagner B, Schmitz HJ, Schrenk D.** Inhibition of apoptosis in rat hepatocytes treated with "non-dioxin-like" polychlorinated biphenyls. *Carcinogenesis* 22: 1601–1606, 2001.
12. **Booker CD, White KL Jr.** Benzo(*a*)pyrene-induced anemia and splenomegaly in NZB/WF1 mice. *Food Chem Toxicol* 43: 1423–1431, 2005.
13. **Bottini E, Gloria-Bottini F, La Torre M, Lucarini N.** The genetics of signal transduction and the effect of smoking on intrauterine growth. *Int J Epidemiol* 30: 400–402, 2001.
14. **Bulay OM, Wattenberg LW.** Carcinogenic effects of subcutaneous administration of benzo(*a*)-pyrene during pregnancy on the progeny. *Proc Soc Exp Biol Med* 135: 84–86, 1970.
15. **Bunger MK, Moran SM, Glover E, Thomae TL, Lahvis GP, Lin BC, Bradfield CA.** Resistance to 2,3,7,8-tetrachlorodibenzo-*p*-dioxin toxicity and abnormal liver development in mice carrying a mutation in the nuclear localization sequence of the aryl hydrocarbon receptor. *J Biol Chem* 278: 17767–17774, 2003.
16. **Burton GJ, Palmer ME, Dalton KJ.** Morphometric differences between the placental vasculature of non-smokers, smokers and ex-smokers. *Br J Obstet Gynaecol* 96: 907–915, 1989.
17. **Bush PG, Mayhew TM, Abramovich DR, Aggett PJ, Burke MD, Page KR.** A quantitative study on the effects of maternal smoking on placental morphology and cadmium concentration. *Placenta* 21: 247–256, 2000.
18. **Carlson DB, Perdew GH.** A dynamic role for the Ah receptor in cell signaling? Insights from a diverse group of Ah receptor interacting proteins. *J Biochem Mol Toxicol* 16: 317–325, 2002.
19. **Carter AM.** Animal models of human placentation—a review. *Placenta* 28, *Suppl* A: S41–S47, 2007.
20. **Cnattingius S.** The epidemiology of smoking during pregnancy: smoking prevalence, maternal characteristics, and pregnancy outcomes. *Nicotine Tob Res* 6, *Suppl* 2: S125–S140, 2004.
21. **Cnattingius S, Lindmark G, Meirik O.** Who continues to smoke while pregnant? *J Epidemiol Community Health* 46: 218–221, 1992.
22. **Cross JC.** How to make a placenta: mechanisms of trophoblast cell differentiation in mice—a review. *Placenta* 26, *Suppl* A: S3–S9, 2005.
23. **Dejmek J, Solansk y I, Podrazilova K, Sram RJ.** The exposure of nonsmoking and smoking mothers to environmental tobacco smoke during different gestational phases and fetal growth. *Environ Health Perspect* 110: 601–606, 2002.
24. **Dempsey D, Jacob P 3rd, Benowitz NL.** Accelerated metabolism of nicotine and cotinine in pregnant smokers. *J Pharmacol Exp Ther* 301: 594–598, 2002.
25. **Denison MS, Heath-Pagliuso S.** The Ah receptor: a regulator of the biochemical and toxicological actions of structurally diverse chemicals. *Bull Environ Contam Toxicol* 61: 557–568, 1998.
26. **Detmar J.** Regulation of cell death during murine placental development and its dysregulation due to xenobiotic exposure. In: *Institute of Medical Sciences*. Toronto: University of Toronto, 2007, p. 1–253.
27. **Detmar J, Rabaglino T, Taniuchi Y, Oh J, Acton BM, Benito A, Nunez G, Jurisicova A.** Embryonic loss due to exposure to polycyclic aromatic hydrocarbons is mediated by Bax. *Apoptosis* 11: 1413–1425, 2006.
28. **Drukteinis JS, Medrano T, Ablordeppey EA, Kitzman JM, Shiverick KT.** Benzo[a]pyrene, but not 2,3,7,8-TCDD, induces G2/M cell cycle arrest, $p21^{CIP1}$ and p53 phosphorylation in human choriocarcinoma JEG-3 cells: a distinct signalling pathway. *Placenta* 26, *Suppl* A: S87–S95, 2005.
29. **England L, Zhang J.** Smoking and risk of preeclampsia: a systematic review. *Front Biosci* 12: 2471–2483, 2007.
30. **England LJ, Grauman A, Qian C, Wilkins DG, Schisterman EF, Yu KF, Levine RJ.** Misclassification of maternal smoking status and its effects on an epidemiologic study of pregnancy outcomes. *Nicotine Tob Res* 9: 1005–1013, 2007.
31. **England LJ, Kendrick JS, Gargiullo PM, Zahniser SC, Hannon WH.** Measures of maternal tobacco exposure and infant birth weight at term. *Am J Epidemiol* 153: 954–960, 2001.
32. **England LJ, Kendrick JS, Wilson HG, Merritt RK, Gargiullo PM, Zahniser SC.** Effects of smoking reduction during pregnancy on the birth weight of term infants. *Am J Epidemiol* 154: 694–701, 2001.
33. **Fernandez-Salguero P, Pineau T, Hilbert DM, McPhail T, Lee SS, Kimura S, Nebert DW, Rudikoff S, Ward JM, Gonzalez FJ.** Immune system impairment and hepatic fibrosis in mice lacking the dioxin-binding Ah receptor. *Science* 268: 722–726, 1995.
34. **Fingerhut LA, Kleinman JC, Kendrick JS.** Smoking before, during, and after pregnancy. *Am J Public Health* 80: 541–544, 1990.
35. **George L, Granath F, Johansson AL, Cnattingius S.** Self-reported nicotine exposure and plasma levels of cotinine in early and late pregnancy. *Acta Obstet Gynecol Scand* 85: 1331–1337, 2006.
36. **Gervais FG, Thornberry NA, Ruffolo SC, Nicholson DW, Roy S.** Caspases cleave focal adhesion kinase during apoptosis to generate a FRNK-like polypeptide. *J Biol Chem* 273: 17102–17108, 1998.
37. **Gladen BC, Zadorozhnaja TD, Chislovska N, Hryhorczuk DO, Kennicutt MC 2nd, Little RE.** Polycyclic aromatic hydrocarbons in placenta. *Hum Exp Toxicol* 19: 597–603, 2000.
38. **Grimmer G, Stober W, Jacob J, Mohr U, Schoene K, Brune H, Misfeld J.** Inventory and biological impact of polycyclic carcinogens in the environment. *Exp Pathol* 24: 3–13, 1983.
39. **Gruslin A, Qiu Q, Tsang BK.** X-linked inhibitor of apoptosis protein expression and the regulation of apoptosis during human placental development. *Biol Reprod* 64: 1264–1272, 2001.
40. **Harris LK, Keogh RJ, Wareing M, Baker PN, Cartwright JE, Aplin JD, Whitley GS.** Invasive trophoblasts stimulate vascular smooth muscle cell apoptosis by a fas ligand-dependent mechanism. *Am J Pathol* 169: 1863–1874, 2006.
41. **Hassoun EA.** In vivo and in vitro interactions of TCDD and other ligands of the Ah-receptor: effect on embryonic and fetal tissues. *Arch Toxicol* 61: 145–149, 1987.
42. **Hegaard HK, Kjaergaard H, Moller LF, Wachmann H, Ottesen B.** Determination of a saliva cotinine cut-off to distinguish pregnant smokers from pregnant non-smokers. *Acta Obstet Gynecol Scand* 86: 401–406, 2007.
43. **Higgins S.** Smoking in pregnancy. *Curr Opin Obstet Gynecol* 14: 145–151, 2002.
44. **Hindmarsh PC, Geary MP, Rodeck CH, Kingdom JC, Cole TJ.** Intrauterine growth and its relationship to size and shape at birth. *Pediatr Res* 52: 263–268, 2002.
45. **Hoffmann D, Hoffmann I.** The changing cigarette, 1950–1995. *J Toxicol Environ Health* 50: 307–364, 1997.
46. **Huppertz B, Kadyrov M, Kingdom JCP.** Apoptosis and its role in the trophoblast. *Am J Obstet Gynecol* 195: 29–39, 2006.
47. **Ishimura R, Kawakami T, Ohsako S, Nohara K, Tohyama C.** Suppressive effect of 2,3,7,8-tetrachlorodibenzo-*p*-dioxin on vascular remodeling that takes place in the normal labyrinth zone of rat placenta during late gestation. *Toxicol Sci* 91: 265–274, 2006.
48. **Kaufmann P, Black S, Huppertz B.** Endovascular trophoblast invasion: implications for the pathogenesis of intrauterine growth retardation and preeclampsia. *Biol Reprod* 69: 1–7, 2003.
49. **Khera KS.** Extraembryonic tissue changes induced by 2,3,7,8-tetrachlorodibenzo-*p*-dioxin and 2,3,4,7,8-pentachlorodibenzofuran with a note on direction of maternal blood flow in the labyrinth of C57BL/6N mice. *Teratology* 45: 611–627, 1992.
50. **Kimya Y, Cengiz C, Ozan H, Kolsal N.** Acute effects of maternal smoking on the uterine and umbilical artery blood velocity waveforms. *J Matern Fetal Investig* 8: 79–81, 1998.
51. **Kitajima M, Khan KN, Fujishita A, Masuzaki H, Koji T, Ishimaru T.** Expression of the arylhydrocarbon receptor in the peri-implantation period of the mouse uterus and the impact of dioxin on mouse implantation. *Arch Histol Cytol* 67: 465–474, 2004.
52. **Larsen LG, Clausen HV, Jonsson L.** Stereologic examination of placentas from mothers who smoke during pregnancy. *Am J Obstet Gynecol* 186: 531–537, 2002.
53. **Leichter J.** Growth of fetuses of rats exposed to ethanol and cigarette smoke during gestation. *Growth Dev Aging* 53: 129–134, 1989.
54. **Lindqvist R, Lendahls L, Tollbom O, Aberg H, Hakansson A.** Smoking during pregnancy: comparison of self-reports and cotinine levels in 496 women. *Acta Obstet Gynecol Scand* 81: 240–244, 2002.

55. **Lu LJ, Disher RM, Reddy MV, Randerath K.** ^{32}P-postlabeling assay in mice of transplacental DNA damage induced by the environmental carcinogens safrole, 4-aminobiphenyl, and benzo(*a*)pyrene. *Cancer Res* 46: 3046–3054, 1986.
56. **Marana HR, Andrade JM, Martins GA, Silva JS, Sala MA, Cunha SP.** A morphometric study of maternal smoking on apoptosis in the syncytiotrophoblast. *Int J Gynaecol Obstet* 61: 21–27, 1998.
57. **Marcoux S, Brisson J, Fabia J.** The effect of cigarette smoking on the risk of preeclampsia and gestational hypertension. *Am J Epidemiol* 130: 950–957, 1989.
58. **Matikainen TM, Moriyama T, Morita Y, Perez GI, Korsmeyer SJ, Sherr DH, Tilly JL.** Ligand activation of the aromatic hydrocarbon receptor transcription factor drives Bax-dependent apoptosis in developing fetal ovarian germ cells. *Endocrinology* 143: 615–620, 2002.
59. **Munafo M, Murphy M, Whiteman D, Hey K.** Does cigarette smoking increase time to conception? *J Biosoc Sci* 34: 65–73, 2002.
60. **Pfarrer C, Macara L, Leiser R, Kingdom J.** Adaptive angiogenesis in placentas of heavy smokers. *Lancet* 354: 303, 1999.
61. **Pocar P, Fischer B, Klonisch T, Hombach-Klonisch S.** Molecular interactions of the aryl hydrocarbon receptor and its biological and toxicological relevance for reproduction. *Reproduction* 129: 379–389, 2005.
62. **Pringle PJ, Geary MP, Rodeck CH, Kingdom JC, Kayamba-Kay's S, Hindmarsh PC.** The influence of cigarette smoking on antenatal growth, birth size, and the insulin-like growth factor axis. *J Clin Endocrinol Metab* 90: 2556–2562, 2005.
63. **Rajini P, Last JA, Pinkerton KE, Hendrickx AG, Witschi H.** Decreased fetal weights in rats exposed to sidestream cigarette smoke. *Fundam Appl Toxicol* 22: 400–404, 1994.
64. **Rees ED, Mandelstam P, Lowry JQ, Lipscomb H.** A study of the mechanism of intestinal absorption of benzo(*a*)pyrene. *Biochim Biophys Acta* 225: 96–107, 1971.
65. **Rennie MY, Whiteley KJ, Kulandavelu S, Adamson SL, Sled JG.** 3D visualisation and quantification by microcomputed tomography of late gestational changes in the arterial and venous feto-placental vasculature of the mouse. *Placenta* 28: 833–840, 2007.
66. **Robles R, Morita Y, Mann KK, Perez GI, Yang S, Matikainen T, Sherr DH, Tilly JL.** The aryl hydrocarbon receptor, a basic helix-loop-helix transcription factor of the PAS gene family, is required for normal ovarian germ cell dynamics in the mouse. *Endocrinology* 141: 450–453, 2000.
67. **Rush D, Kristal A, Blanc W, Navarro C, Chauhan P, Campbell Brown M, Rosso P, Winick M, Brasel J, Naeye R, Susser M.** The effects of maternal cigarette smoking on placental morphology, histomorphometry, and biochemistry. *Am J Perinatol* 3: 263–272, 1986.
68. **Salafia C, Shiverick K.** Cigarette smoking and pregnancy II: vascular effects. *Placenta* 20: 273–279, 1999.
69. **Salafia CM, Zhang J, Charles AK, Bresnahan M, Shrout P, Sun W, Maas EM.** Placental characteristics and birthweight. *Paediatr Perinat Epidemiol* 22: 229–239, 2008.
70. **Schmidt JV, Su GH, Reddy JK, Simon MC, Bradfield CA.** Characterization of a murine Ahr null allele: involvement of the Ah receptor in hepatic growth and development. *Proc Natl Acad Sci USA* 93: 6731–6736, 1996.
71. **Shimizu Y, Nakatsuru Y, Ichinose M, Takahashi Y, Kume H, Mimura J, Fujii-Kuriyama Y, Ishikawa T.** Benzo[*a*]pyrene carcinogenicity is lost in mice lacking the aryl hydrocarbon receptor. *Proc Natl Acad Sci USA* 97: 779–782, 2000.
72. **Shiverick KT, Salafia C.** Cigarette smoking and pregnancy I: ovarian, uterine and placental effects. *Placenta* 20: 265–272, 1999.
73. **Shugart L, Matsunami R.** Adduct formation in hemoglobin of the newborn mouse exposed in utero to benzo[*a*]pyrene. *Toxicology* 37: 241–245, 1985.
74. **Singh NP, Nagarkatti M, Nagarkatti PS.** Role of dioxin response element and nuclear factor-kappaB motifs in 2,3,7,8-tetrachlorodibenzo-*p*-dioxin-mediated regulation of Fas and Fas ligand expression. *Mol Pharmacol* 71: 145–157, 2007.
75. **Stavenow L, Pessah-Rasmussen H.** Effects of polycyclic aromatic hydrocarbons on proliferation, collagen secretion and viability of arterial smooth muscle cells in culture. *Artery* 15: 94–108, 1988.
76. **Straszewski-Chavez SL, Abrahams VM, Mor G.** The role of apoptosis in the regulation of trophoblast survival and differentiation during pregnancy. *Endocr Rev* 26: 877–897, 2005.
77. **Suzuki M, Aoshiba K, Nagai A.** Oxidative stress increases Fas ligand expression in endothelial cells. *J Inflamm (Lond)* 3: 11, 2006.
78. **Thackaberry EA, Gabaldon DM, Walker MK, Smith SM.** Aryl hydrocarbon receptor null mice develop cardiac hypertrophy and increased hypoxia-inducible factor-1alpha in the absence of cardiac hypoxia. *Cardiovasc Toxicol* 2: 263–274, 2002.
79. **Torres J, Rodriguez J, Myers MP, Valiente M, Graves JD, Tonks NK, Pulido R.** Phosphorylation-regulated cleavage of the tumor suppressor PTEN by caspase-3: implications for the control of protein stability and PTEN-protein interactions. *J Biol Chem* 278: 30652–30660, 2003.
80. **Usmani ZC, Craig P, Shipton D, Tappin D.** Comparison of CO breath testing and women's self-reporting of smoking behaviour for identifying smoking during pregnancy. *Subst Abuse Treat Prev Policy* 3: 4, 2008.
81. **van der Veen F, Fox H.** The effects of cigarette smoking on the human placenta: a light and electron microscopic study. *Placenta* 3: 243–256, 1982.
82. **Wang X, Ding H, Ryan L, Xu X.** Association between air pollution and low birth weight: a community-based study. *Environ Health Perspect* 105: 514–520, 1997.
83. **Weber H, Harris MW, Haseman JK, Birnbaum LS.** Teratogenic potency of TCDD, TCDF and TCDD-TCDF combinations in C57BL/6N mice. *Toxicol Lett* 26: 159–167, 1985.
84. **Windham GC, Hopkins B, Fenster L, Swan SH.** Prenatal active or passive tobacco smoke exposure and the risk of preterm delivery or low birth weight. *Epidemiology* 11: 427–433, 2000.
85. **Woo M, Hakem R, Furlonger C, Hakem A, Duncan GS, Sasaki T, Bouchard D, Lu L, Wu GE, Paige CJ, Mak TW.** Caspase-3 regulates cell cycle in B cells: a consequence of substrate specificity. *Nat Immunol* 4: 1016–1022, 2003.
86. **Woodruff TJ, Grillo J, Schoendorf KC.** The relationship between selected causes of postneonatal infant mortality and particulate air pollution in the United States. *Environ Health Perspect* 105: 608–612, 1997.
87. **Yang J, Jones SP, Suhara T, Greer JJ, Ware PD, Nguyen NP, Perlman H, Nelson DP, Lefer DJ, Walsh K.** Endothelial cell overexpression of fas ligand attenuates ischemia-reperfusion injury in the heart. *J Biol Chem* 278: 15185–15191, 2003.
88. **Yin L, Morita A, Tsuji T.** Alterations of extracellular matrix induced by tobacco smoke extract. *Arch Dermatol Res* 292: 188–194, 2000.
89. **Yin L, Morita A, Tsuji T.** Tobacco smoke extract induces age-related changes due to modulation of TGF-beta. *Exp Dermatol* 12, *Suppl* 2: 51–56, 2003.
90. **Zhang L, Shiverick KT.** Differential effects of 2,3,7,8-tetrachlorodibenzo-*p*-dioxin and benzo(*a*)pyrene on proliferation and growth factor expression in human choriocarcinoma BeWo cells. *Trophoblast Res* 11: 177–191, 1998.